

A key point here is that these results clearly demonstrate that a small nonsurfactant organic molecule can reside in at least two distinctively different environments within the bilayer vesicle and that exchange between these sites *below* the phase transition temperature is slow ( $k < 10^{-4} \text{ s}^{-1}$ ) on the photochemical time scale.

**Acknowledgment.** We are grateful to the National Science Foundation (Grant CHE 8315303) for support of this research.

**Registry No.** NMS, 1472-68-0; SDS, 151-21-3; CTAB, 57-09-0; Brij-35, 9002-92-0; DPL, 2644-64-6; DODAC, 107-64-2; DCP, 2197-63-9.

### Optical Microscopic Study of Helical Superstructures of Chiral Bilayer Membranes

Naotoshi Nakashima, Sumitoshi Asakuma, and Toyoki Kunitake\*

*Contribution No. 745, Department of Organic Synthesis, Faculty of Engineering Kyushu University, Fukuoka 812, Japan*

*Received September 10, 1984*

We describe in the paper the direct observation of helical superstructures produced from bilayer membranes of chiral ammonium amphiphiles.

Recently, we conducted direct observation of aqueous dispersions of synthetic bilayer membranes by using dark-field optical microscopy.<sup>1</sup> Their morphologies were often very different from what we observe by electron microscopy. When bilayer membranes are in the liquid-crystalline (fluid) state, a variety of dynamically changing morphologies such as fibers, tubules, twisted vesicles, etc. are observed. This suggests that shapes of bilayer aggregates are far richer than expected from the electron microscopic (static) observation and clearly points to the advantage of the direct observation. Some amino acid derived amphiphiles produce well-developed bilayer membranes that display remarkable enhancements of circular dichroism<sup>2,3</sup> and induced circular dichroism.<sup>4</sup> These results were an indication of the existence of regular superstructures and prompted us to examine these bilayers by optical microscopy.

Double-chain ammonium amphiphiles given in Chart I produce typical bilayer vesicles, when dispersed in water by sonication.<sup>5</sup> One milligram of these amphiphiles were added to 1 mL of water, allowed to swell by warming, and shaken gently by hand. Transparent dispersions thus obtained were placed on slide glass and were observed by a dark-field light microscope (Olympus BHF, light source; Ushio 200-W high-pressure Hg lamp). When an aqueous dispersion of  $2\text{C}_{12}\text{-L-Glu-C}_{11}\text{N}^+$  is maintained at 20 °C for several hours, flexible filaments of lengths of 5–50  $\mu\text{m}$  are formed predominantly (Figure 1a). Spherical vesicles (diameter, 1–10  $\mu\text{m}$ ) are present as a minor component. These aggregates show rapid Brownian motions. Upon aging at 15–20 °C for 1 day, the filaments begin to be twisted. It takes several hours for one filament to change completely into a helix such as shown in Figure 1b. The scattering from helices is intensified over a period of 5–6 h (Figure 1c). The helical pitches are similar (ca. 3.2  $\mu\text{m}$ ) in Figure 1, parts b and c, and lengths of the helix are 10–100  $\mu\text{m}$ . Some helices are bent. Further shape changes occur more gradually, and after 1 month, rodlike structures become abundant (Figure 1d).

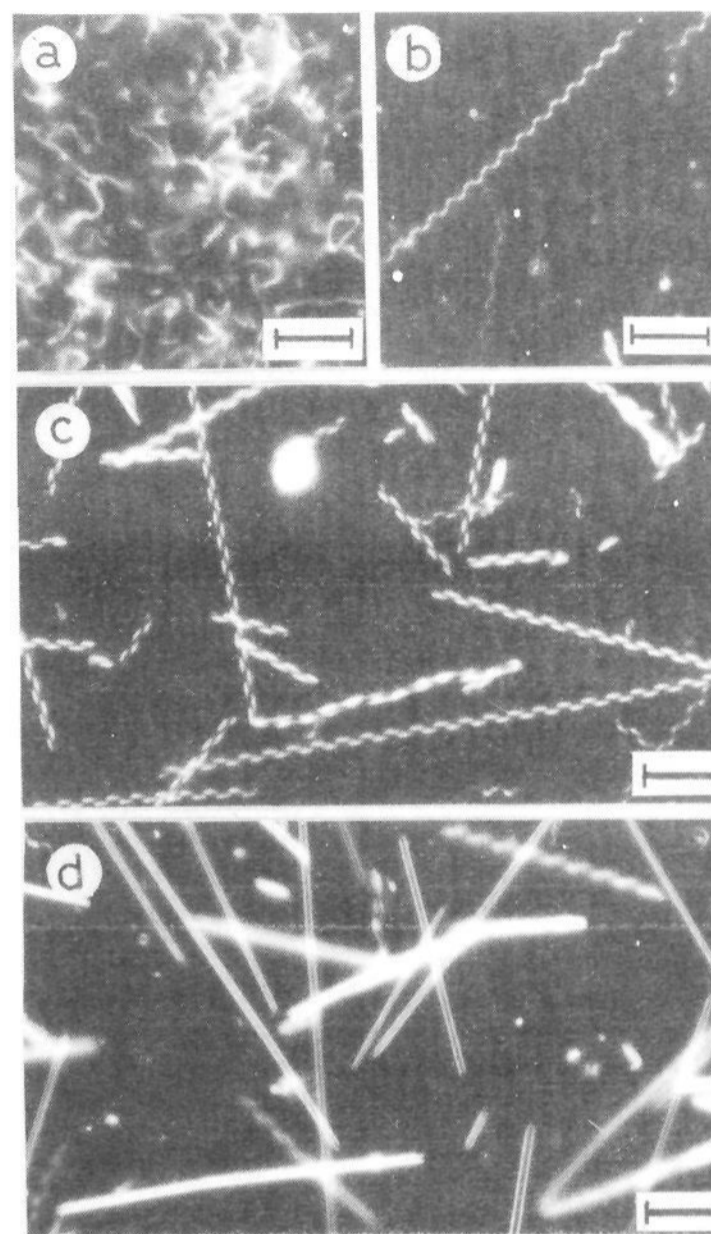


**Figure 1.** Dark-field optical micrographs of aqueous dispersion of  $2\text{C}_{12}\text{-L-Glu-C}_{11}\text{N}^+$  ( $1 \times 10^{-3} \text{ M}$ ). Micrographs (a)–(d) show the growth from fibrous chiral bilayers to helical superstructures. Aging condition: (a) 20 °C, several hours; (b) 15–20 °C, 1 day; (c) 5–6 h after b; (d) 15–20 °C, 1 month. Magnification 1300 times (scale bars, 10  $\mu\text{m}$ ).

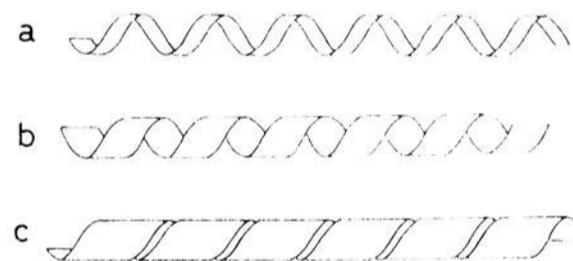
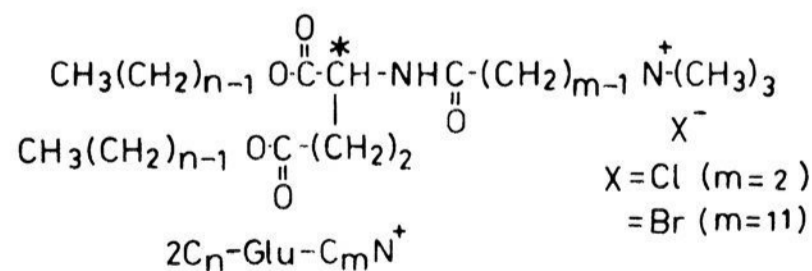


**Figure 2.** Schematic illustrations of the growing process of a helix. (a), (b), and (c) are illustrations approximately corresponding to Figure 1, parts b, c, and d, respectively.

#### Chart I



- |   |  |
|---|--|
| 1, $2\text{C}_{12}\text{-L-Glu-C}_2\text{N}^+$    | 2, $2\text{C}_{12}\text{-L-Glu-C}_{11}\text{N}^+$  |
| 3, $2\text{C}_{12}\text{-D-Glu-C}_{11}\text{N}^+$ | 4, $2\text{C}_{12}\text{-DL-Glu-C}_{11}\text{N}^+$ |
| 5, $2\text{C}_{14}\text{-L-Glu-C}_2\text{N}^+$    | 6, $2\text{C}_{14}\text{-L-Glu-C}_{11}\text{N}^+$  |

The growing processes are schematically illustrated in Figure 2. The pitches of the twisted tapes are identical; therefore, the changes from helices of narrow tapes (Figures 2a and 1b) to rods (Figures 2c and 1d) probably occur via widening of the tape.<sup>6</sup>

(1) Nakashima, N.; Asakuma, S.; Kunitake, T.; Hotani, H. *Chem. Lett.* **1984**, 227–230.

(2) Kunitake, T.; Nakashima, N.; Shimomura, M.; Okahata, Y.; Kano, K.; Ogawa, T. *J. Am. Chem. Soc.* **1980**, *102*, 6642–6644.

(3) Kunitake, T.; Nakashima, N.; Morimitsu, K. *Chem. Lett.* **1980**, 1347–1350.

(4) Nakashima, N.; Fukushima, H.; Kunitake, T. *Chem. Lett.* **1981**, 1207–1210.

(5) Nakashima, N.; Asakuma, S.; Kunitake, T. *Chem. Lett.* **1984**, 1709–1712.

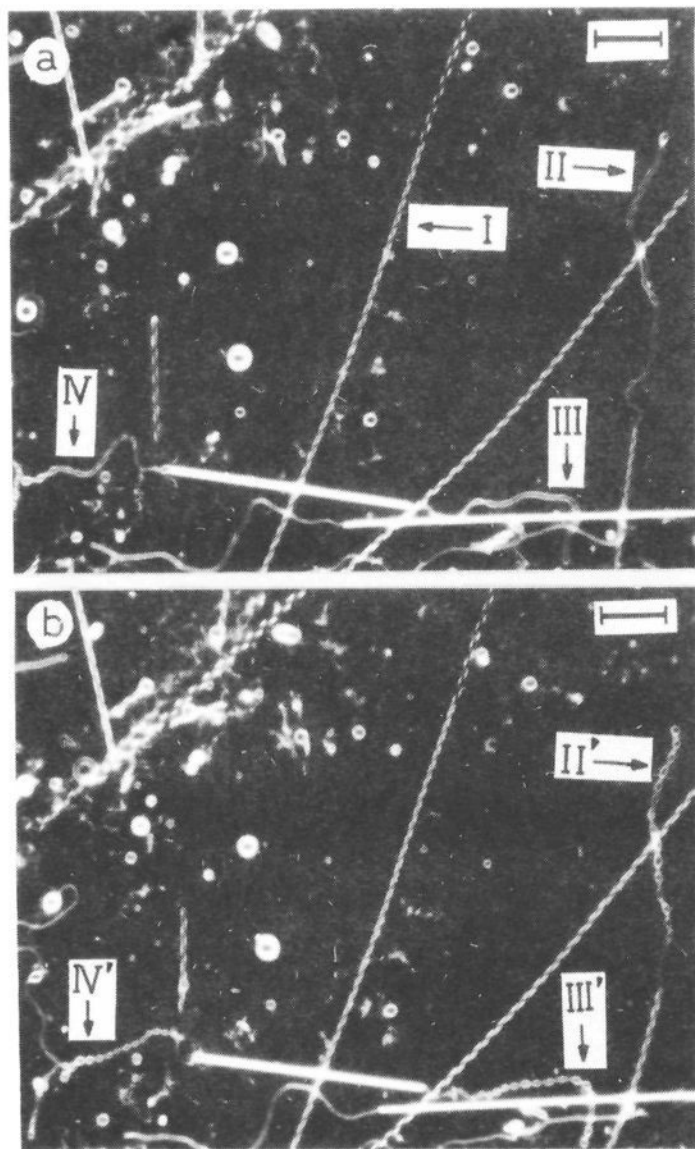


**Figure 3.** Shape changes of helices into vesicles via tubular structures.  $2C_{12}$ -L-Glu- $C_{11}N^+$ ,  $1 \times 10^{-3}$  M. Micrographs (a) and (b) are obtained within an interval of 1 s during slow heating of the solution beyond  $T_c$ . Noticeable shape changes are denoted by arrows. Magnification 1300 times (scale bars, 10  $\mu$ m).

Enantiomeric  $2C_{12}$ -D-Glu- $C_{11}N^+$  produces similar helical structures. The sense of the helix of the L amphiphile is always right handed, and that of the D amphiphile is left handed. They do not change, even when the helix is bent. Helices are not found for aqueous dispersions of racemic  $2C_{12}$ -DL-Glu- $C_{11}N^+$ ; instead, elastic fibers are present.

The helical superstructures are stable only at temperatures below the phase transition temperature ( $T_c$ ) of the respective bilayers ( $T_c = 34$  °C for helical  $2C_{12}$ -L-Glu- $C_{11}N^+$ ).<sup>5</sup> The helices of Figure 1 change instantaneously to spherical vesicles and flexible filaments, when the solution is warmed to 40–50 °C. The conversion processes can be seen more clearly by slower heating. At temperatures near  $T_c$ , the pitch of a long helix of  $2C_{12}$ -L-Glu- $C_{11}N^+$  becomes shorter (from 3.2 to 2.8  $\mu$ m) from one end (Figure 3a, I). The helices are then transformed into tubes (Figure 3a, II), which are immediately constricted and separated into vesicles. Figure 3, parts a and b are photographed within an interval of 1 s, and the rapid constriction process is apparent from comparisons of II with II', III with III', and IV with IV'. Some flexible filaments remain intact. All helices are eventually transformed into vesicles or flexible filaments.

The chemical structure of component amphiphiles in addition to their chirality plays crucial roles in morphology.  $2C_{14}$ -L-Glu- $C_{11}N^+$  gives helical aggregates, whereas  $2C_{12}$ -L-Glu- $C_2N^+$  and  $2C_{14}$ -L-Glu- $C_2N^+$  form spherical vesicles (diameter, several micrometers) at all temperatures. Long spacer methylenes ( $C_m$ ) are required for helix formation.

It is known that biological lipids (lecithins) form helical myelin figures.<sup>7–9</sup> Lin et al. reported the induction of helical liposomes

by  $Ca^{2+}$ , and Sakurai and Kawamura studied the growth mechanism of myelin figures. These results are in sharp contrast with ours in that helices are formed only in the chain-melting phase (above  $T_c$ ) and do not exhibit enantiomorphism.

Recently, however, Weis et al.<sup>10</sup> reported two-dimensional chiral crystals of phospholipid at the air/water interface. In the case of non-bilayer-forming amphiphiles, helix formation has already been reported from 12-hydroxystearic acid, both in organic gel state<sup>11,12</sup> and from a collapsed monolayer.<sup>13–15</sup>

In conclusion, helical superstructures are formed from synthetic, chiral bilayer membranes. The physical state and the chemical structure are crucial for generation and transformation of these helices. It is now possible to prepare helical superstructures from *designed* component amphiphiles. Electron microscopic studies of these and related systems are published elsewhere.<sup>5,16</sup>

**Acknowledgment.** We are grateful to Dr. Hirokazu Hotani of Kyoto University for his helpful discussion. The present study was supported in part by Special Coordination Funds for Promoting Science and Technology from Science and Technology Agency of Japan.

**Registry No.** 1, 94061-40-2; 2, 93965-91-4; 3, 93965-92-5; 4, 93965-93-6; 5, 93965-94-7; 6, 93965-95-8.

(8) Lin, K.-C.; Weis, R. M.; McConnell, H. M. *Nature (London)* **1982**, 296, 164–165.

(9) Sakurai, I.; Kawamura, Y., personal communication.

(10) Weis, R. M.; McConnell, H. M. *Nature (London)* **1984**, 310, 47–50.

(11) Tachibana, T.; Kayama, K.; Takeno, H. *Bull. Chem. Soc. Jpn.* **1969**, 42, 3422–3424.

(12) Uzu, Y.; Sugiura, T. *J. Colloid Interface Sci.* **1975**, 51, 346–349.

(13) Tachibana, T.; Hori, K. *J. Colloid Interface Sci.* **1977**, 61, 398–400.

(14) Tachibana, T.; Yoshizumi, T.; Hori, K. *Bull. Chem. Soc. Jpn.* **1979**, 52, 34–41.

(15) Stewart, M. V.; Arnett, E. M. *Top. Stereochem.* **1982**, 13, 195–262.

(16) Yamada, K.; Ihara, H.; Ide, T.; Fukumoto, T.; Hirayama, C. *Chem. Lett.* **1984**, 1713–1716.

### Magnetic and Spectroscopic Properties of the $\delta\delta^*$ Excited States of $Mo_2Cl_4(PMe_3)_4$ and $\beta$ - $Mo_2Cl_4(Me_2PCH_2CH_2PMe_2)_2$ : Experimental Determination of the Energy of a Triplet $\delta\delta^*$ State

Michael D. Hopkins,\* Thomas C. Zietlow,  
Vincent M. Miskowski, and Harry B. Gray\*

Contribution No. 7100, Arthur Amos Noyes Laboratory  
California Institute of Technology  
Pasadena, California 91125

Received September 20, 1984

The lowest lying electronic excited state of complexes containing quadruple metal–metal bonds is a spin triplet of configuration  $[\sigma^2\pi^4\delta\delta^*]$ . Although the energy of this state has yet to be directly determined by magnetic or spectroscopic measurements, simple theoretical considerations of weakly interacting orbitals,<sup>1–3</sup> as well as indirect experimental evidence,<sup>1,4</sup> suggest that it lies much closer to the ( $\delta^2$ ) ground state than to its singlet ( $\delta\delta^*$ ) counterpart. Ab initio generalized valence bond calculations on  $Re_2Cl_8^{2-}$  have borne this out, placing the  $^3(\delta\delta^*)$  state of this complex 3200  $cm^{-1}$  above the ground state and 11 200  $cm^{-1}$  below  $^1(\delta\delta^*)$ .<sup>5</sup> Over the past several years, a number of  $d^4$ – $d^4$  dimers have been reported in

(1) Miskowski, V. M.; Goldbeck, R. A.; Kliger, D. S.; Gray, H. B. *Inorg. Chem.* **1979**, 18, 86–89.

(2) Hay, P. J.; Thibeault, J. C.; Hoffmann, R. *J. Am. Chem. Soc.* **1975**, 97, 4884–4899.

(3) Hansen, A. E.; Ballhausen, C. J. *Trans. Faraday Soc.* **1965**, 61, 631–639.

(4) Zietlow, T. C.; Hopkins, M. D.; Gray, H. B. *J. Solid State Chem.*, in press.

(5) Hay, P. J. *J. Am. Chem. Soc.* **1982**, 104, 7007–7017.

(6) Another possible mechanism for this transformation is the double-helix formation.

(7) Virchow, R. *Virchows Arch Pathol. Anat. Physiol.* **1854**, 6, 571. Cited in Kelker, H. *Mol. Cryst. Liq. Cryst.* **1973**, 21, 1–48.